to rate their present happiness states using a 7-point scale, and blood samples were collected before and after warm partner contact. ANOVA revealed significant interactions between the condition (control or warm contact) and period (before or after) for the rating score of happiness ($F(1,26) = 2.57$, $p<0.05$, Figure 1B). Further analyses using the paired $t$ test revealed that the rating score for happiness increased significantly ($df = 13$, $t = -2.28$, $p<0.05$) after warm partner contact. Subsequently, we analyzed changes in pro-inflammatory cytokine levels after warm partner contact. Interestingly, ANOVA revealed a significant main effect of the period on the concentration of IFN-γ in the serum ($F(1,26) = 10.37$, $p<0.01$, Figure 1C). Further analyses using the paired $t$ test revealed that the IFN-γ concentration decreased significantly ($df = 13$, $t = 3.21$, $p<0.01$) after warm partner contact, whereas it did not change in the control condition. No significant differences were observed regarding IL-6 and TNF-α levels (data not shown).

## DISCUSSION

We first hypothesized that the level of perceived happiness may be associated with systemic inflammation and negatively correlated with peripheral circulating pro-inflammatory cytokines. As expected, the IFN-γ concentration was lower and health-related QOL was higher in individuals with high-perceived happiness than in individuals with low-perceived happiness. The IFN-γ concentration was negatively correlated with the level of perceived happiness. It is known that the elevation of IFN-γ decreases serotonin levels though the modulation of IDO activity; therefore, serotonin may be abundant in the brains of individuals with high-perceived happiness compared to those with low-perceived happiness. Increased serotonin levels may enhance the reactivity toward positive stimuli. A previous study demonstrated that antidepressant treatment enhances amygdala response to happy faces (Norbury *et al.* 2009). Our previous study also demonstrated that the short form of the serotonin transporter gene-linked polymorphic region, which increases serotonin secretion from presynaptic neurons through reduced serotonin reuptake, also enhances amygdala response to desired persons (Matsunaga *et al.* 2010). When IFN-γ levels decrease, the reactivity to positive stimuli increases, and consequently, the evocation of happiness is enhanced.

We subsequently assessed whether experimentally induced happiness could decrease circulating IFN-γ levels. In this study, we used warm physical contact toward the love partner as the happiness inducer. Interestingly, warm partner contact reduced serum IFN-γ concentrations concurrently with the evocation of happiness. The biological mechanism explaining this phenomenon is still under speculation. Happiness is a positive feeling characterized by contentment, satisfaction, joy, pleasure, or love. Dopamine plays an important role in the expression of positive emotions (Aron *et al.* 2005; Bartels & Zeki 2004; Verhoeff *et al.* 2003). The dopaminergic network within the brain, which projects to the prefrontal cortex and striatum from the midbrain region, is known as the "brain reward system" (Aron *et al.* 2005; Bartels & Zeki 2004), and our previous study demonstrated that the brain reward system is associated with levels of perceived happiness (Matsunaga *et al.* 2011). An interaction between dopamine and IFN-γ was previously observed, and the activation of dopamine receptors by dopamine receptor agonists could suppress the production of IFN-γ in T-lymphocytes, which are known to be major producers of IFN-γ (Huang *et al.* 2010). Therefore, it is possible that experimentally induced happiness decreases IFN-γ production through dopamine-dependent mechanisms.

Previous psychoneuroimmunologic studies revealed an association between other inflammatory markers and positive emotional states. It has been demonstrated that higher positive well-being was associated with lower plasma IL-6 levels (Steptoe *et al.* 2009). In addition to IFN-γ, peripheral IL-6 can also reach the brain via leaky regions in the blood-brain barrier, active transport molecules, and afferent nerve fibers. Recent neuroimaging studies directly revealed that vaccination-induced peripheral IL-6 elevation decreased cognitive function through modulation of the activities of several brain regions, such as the insula and anterior cingulate cortex (Harrison *et al.* 2009). These brain regions are also known to be involved in emotional perception (Matsunaga *et al.* 2009b). We investigated the association between levels of perceived happiness and those of peripheral IL-6 in this study; unfortunately, we did not observe an interaction between these 2 variables. Although we cannot deny the possibility that IFN-γ and IL-6 influence different feelings, one of the reasons why we could not detect an interaction between the levels of perceived happiness and those of other pro-inflammatory cytokines may be the relatively small sample size ($n = 160$). Thus, the generalizability of the current findings should be further tested by using larger samples. Nevertheless, the present study demonstrated that the level of perceived happiness influences the levels of peripheral circulating pro-inflammatory cytokines. These results may expand the scope of clinical literature that addresses the links between positive emotions and immunity.

## ACKNOWLEDGEMENTS

This work was supported by a Grant-in-Aid for Young Scientists (B) from the Japan Society for the Promotion of Science (JSPS) (22700683 to MM).

***Conflict of Interest Statement***

*The authors have no conflicts of interest to declare.*

REFERENCES


1 Ader R (2000) On the development of psychoneuroimmunology. Eur J Pharmacol. **405**: 167–176.
2 Aron A, Fisher H, Mashek DJ, Strong G, Li H, Brown LL (2005) Reward, motivation, and emotion systems associated with early-stage intense romantic love. J Neurophysiol. **94**: 327–337.
3 Bartels A, Zeki S (2004) The neural correlates of maternal and romantic love. NeuroImage. **21**: 1155–1166.
4 Bosch JA, Berntson GG, Cacioppo JT, Marucha PT (2005) Differential mobilization of functionally distinct natural killer subsets during acute psychologic stress. Psychosomatic Medicine. **67**: 366–75.
5 Dantzer R, O'Connor JC, Freund GG, Johnson RW, Kelley KW (2008) From inflammation to sickness and depression: when the immune system subjugates the brain. Nat Rev Neurosci. **9**: 46–56 (Review).
6 Fukuhara S, Bito S, Green J, Hsiao A, Kurokawa K (1998a) Translation, adaptation, and validation of the SF-36 Health Survey for use in Japan. J Clin Epidemiol. **51**: 1037–1044.
7 Fukuhara S, Ware JE, Kosinski M, Wada S, Gandek B (1998b) Psychometric and clinical tests of validity of the Japanese SF-36 Health Survey. J Clin Epidemiol. **51**: 1045–1053.
8 Hamer M, Stamatakis E (2008) The accumulative effects of modifiable risk factors on inflammation and haemostasis. Brain Behav Immunity. **22**: 1041–1043.
9 Harrison NA, Brydon L, Walker C, Gray MA, Steptoe A, Dolan RJ, Critchley HD (2009) Neural origins of human sickness in interoceptive responses to inflammation. Biol. Psychiatry. **66**: 415–422.
10 Hatfield E, Sprecher S (1986) Measuring passionate love in intimate relationships. J Adolesc. **9**: 383–410.
11 Horiuchi S, Tsuda A, Hashimoto E, Kai H, Wenjie H (2008) Effect of perceived happiness level on cardiac response to mental stress testing: A pilot study. Japan J Biofeedback Res. **35**: 93–98.
12 Huang Y, Qiu A, Peng Y, Liu Y, Huang H, Qiu Y (2010) Roles of dopamine receptor subtypes in mediating modulation of T lymphocyte function. Neuroendocrinol Lett. **31**: 782–791.
13 Maes M, Kubera M, Obuchowiczwa E, Goehler L, Brzeszcz J (2011) Depression's multiple comorbidities explained by (neuro)inflammatory and oxidative & nitrosative stress pathways. Neuro Endocrinol Lett. **32**: 7–24.
14 Magalhaes AC, Holmes KD, Dale LB, Comps-Agrar L, Lee D, Yadav PN, Drysdale L, Poulter MO, Roth BL, Pin JP, Anisman H, Ferguson SS (2010) CRF receptor 1 regulates anxiety behavior via sensitization of 5-HT2 receptor signaling. Nat Neurosci.**13**: 622–629.
15 Matsunaga M, Sato S, Isowa T, Tsuboi H, Konagaya T, Kaneko H, Ohira H (2009a) Profiling of serum proteins influenced by warm partner contact in healthy couples. Neuroendocrinol Lett. **30**: 227–36.
16 Matsunaga M, Isowa T, Kimura K, Miyakoshi M, Kanayama N, Murakami H, Fukuyama S, Shinoda J, Yamada J, Konagaya T, Kaneko H, Ohira H (2009b) Associations among positive mood, brain, and cardiovascular activities in an affectively positive situation. Brain Res. **1263**: 93–103.
17 Matsunaga M, Murakami H, Yamakawa K, Isowa T, Kasugai K, Yoneda M, Kaneko H, Fukuyama S, Shinoda J, Yamada J, Ohira H (2010) Genetic variations in the serotonin transporter gene-linked polymorphic region influence attraction for a favorite person and the associated interactions between the central nervous and immune systems. Neurosci Lett. **468**: 211–215.
18 Matsunaga M, Murakami H, Yamakawa K, Isowa T, Fukuyama S, Shinoda J, Yamada J, Ohira H (2011) Perceived happiness level influences positive emotion evocation. Natural Science. **3**: 723–727.
19 Norbury R, Taylor MJ, Selvaraj S, Murphy SE, Harmer CJ, Cowen PJ (2009) Short-term antidepressant treatment modulates amygdala response to happy faces. Psychopharmacology **206**: 197–204.
20 Odamaki M, Kato A, Kumagai H, Hishida A (2004) Counter-regulatory effects of procalcitonin and indoxyl sulphate on net albumin secretion by cultured rat hepatocytes. Nephrol Dial Transplant. **19**: 797–804.
21 Pan A, Ye X, Franco OH, Li H, Yu Z, Wang J, Qi Q, Gu W, Pang X, Liu H, Lin X (2008) The association of depressive symptoms with inflammatory factors and adipokines in middle-aged and older Chinese. PLoS One. **3**: e1392.
22 Raison CL, Capuron L, Miller AH (2006) Cytokines sing the blues: inflammation and the pathogenesis of depression. Trends Immunol. **27**: 24–31 (Review).
23 Shimai S, Otake K, Utsuki N, Ikemi A, Lyubomirsky S (2004) Development of a Japanese version of the subjective happiness scale (SHS), and examination of its validity and reliability. Japan J of Public Health. **51**: 845–853.
24 Steptoe A, Dockray S, Wardle J (2009) Positive affect and psychobiological processes relevant to health. J Pers. **77**: 1747–1776 (Review).
25 Verhoeff NP, Christensen BK, Hussey D, Lee M, Papatheodorou G, Kopala L, Rui Q, Zipursky RB, Kapur S (2003) Effects of catecholamine depletion on D2 receptor binding, mood, and attentiveness in humans: a replication study. Pharmacol Biochem Behav. **74**: 425–432.

Original Paper

Digestion

Digestion 2011;84:253–260
DOI: 10.1159/000330843

Received: December 14, 2010
Accepted: July 15, 2011
Published online: September 22, 2011

# Usefulness of a Slow Nutrient Drinking Test for Evaluating Gastric Perception and Accommodation

Akihito Iida[a] Toshihiro Konagaya[b] Hiroshi Kaneko[c] Yasushi Funaki[a]
Tamotsu Kanazawa[a] Kentaro Tokudome[a] Yasutaka Hijikata[a] Ryuta Masui[a]
Naotaka Ogasawara[a] Makoto Sasaki[a] Masashi Yoneda[a] Kunio Kasugai[a]

[a]Division of Gastroenterology, Department of Internal Medicine, Aichi Medical University School of Medicine, Nagakute, [b]Marine Clinic and Department of Gastroenterology, Nagoya University Graduate School of Medicine, and [c]Department of Neurology (Psychosomatic Medicine), Banbuntane-Hotokukai Hospital, Fujita Health University School of Medicine, Nagoya, Japan

**Key Words**
Gastric barostat · Accommodation volume · Perception · Nutrient drinking test · Mosapride citrate · Placebo-controlled double-blind study

**Abstract**
***Background/Aim:*** An implication of the drinking test for gastric function is controversial. We evaluated the usefulness of a nutrient drinking test for examining gastric function by comparing it with a gastric barostat study. ***Methods:*** We investigated perceived pressure of an intragastric bag with stepwise distension and postprandial peak gastric volume (accommodation volume) with a consistent pressure after drinking a liquid meal (200 ml, 300 kcal) in 18 volunteers. Drinking a similar liquid meal on a different day at a continual rate of 15 ml/min was performed to score satiety and bloated sensations at 5-min intervals. An additional 10 volunteers performed the drinking test before and after administration of mosapride citrate or a placebo in a double-blind crossover study. ***Results:*** Pressure to induce severe discomfort correlated positively with maximum satiety volume in the drinking test (r = 0.60, p = 0.02). Accommodation volume in the barostat study showed a significant correlation (r = 0.59, p = 0.03) with threshold volume to induce bloating in the drinking test. Mosapride tended to increase the volume inducing the first bloated sensation as compared to the placebo. ***Conclusion:*** The present drinking test may be useful for evaluating the threshold to induce severe discomfort and accommodation volume.


## Introduction

According to Rome III, the classification for functional gastrointestinal disorders published in 2006, functional dyspepsia (FD) is defined as the presence of one or more dyspepsia symptoms (postprandial fullness, early satiation, epigastric pain and epigastric burning) that originate from the gastroduodenal region in the absence of any organic, systemic or metabolic disease that is likely to explain the symptoms [1]. Alteration of gastric motility, visceral hypersensitivity, impaired accommodation of meals, gastritis induced by *Helicobacter pylori* infection and dysfunction of the central nervous system have

KARGER
Fax +41 61 306 12 34
E-Mail karger@karger.ch
www.karger.com


0012–2823/11/0844–0253$38.00/0

Accessible online at:
www.karger.com/dig

Akihito Iida, MD
Division of Gastroenterology, Department of Internal Medicine
Aichi Medical University School of Medicine
21 Karimata, Yazako, Nagakute, Aichi 480-1195 (Japan)
Tel. +81 561 62 3311, E-Mail iida@aichi-med-u.ac.jp

all been implicated in the pathophysiology of FD [2, 3]. A pathophysiology-based treatment strategy has been recommended; therefore, acceptable tests for measuring gut function have been intensively investigated.

The gastric barostat study is the gold standard method for evaluating gastric perception and accommodation [4–6], despite some criticism [7]. However, this technique has serious drawbacks, such as expense and invasiveness. In fact, barostat studies have only been conducted in a few institutions around the world, including Japan.

Several drinking tests have been developed in Western countries as noninvasive methods to assess gastric perception and accommodation [4–6, 8–10]. Recently, Japanese researchers developed a novel drinking-ultrasonography (US) test to assess gastric motility and sensory function [11]. Such tests are easily performed without special instruments and are well tolerated. The initial study of the satiety drinking test reported in 1998 by Tack et al. [4] demonstrated a good correlation with the results of barostat studies in the dyspepsia patients. Recently, good reproducibility of the drinking test has been shown [12]. In contrast, other investigators have found that drinking tests are a less sensitive predictor of impaired accommodation or visceral hypersensitivity than the barostat study [13]. No data are available on the usefulness of drinking tests in comparison with the gold standard method, the barostat, in Japan. The primary aim of the present study was to compare the slow nutrient drinking test with the barostat method in volunteers.

Mosapride citrate, a 5-hydroxytryptamine-4 (5-HT4) agonist [14], is an effective drug for dyspeptic symptoms in oriental countries [15, 16]. This compound reportedly enhances gastric accommodation, as determined by US, in Japanese normal volunteers [17]. Thus, the secondary aim of this study was to investigate the effects of mosapride on gastric accommodation determined by the present nutrient drinking test.

## Subjects and Methods

*Study Subjects*

To compare the slow nutrient drinking test with the barostat method, 18 male volunteers (mean age: 31.3 ± 5.4 years; range: 25–44) participated. Another 10 volunteers (mean age: 37.4 ± 2.6 years; range: 25–50) participated in the additional mosapride study. None of the subjects had any history of gastrointestinal disease, nor were they taking any medications. Written informed consent was obtained from each participant. The Ethics Committee of Aichi Medical University approved all the study protocols.

*Gastric Barostat*

The barostat system was set up as reported previously [4, 5]. Following fasting for 12 h, a double lumen polyvinyl tube with an adherent finely folded plastic bag (Mui Scientific, Mississauga, Ont., Canada) was introduced through the mouth into the stomach under fluorography. The polyvinyl tube was then connected to a barostat device (Distender series II™; G&J Electronics, North York, Ont., Canada). The bag was unfolded by inflation of 300 ml of air and was positioned in the proximal stomach in a recumbent position, after which the bag was again deflated. Subjects were then positioned in a comfortable sitting position with knees bent (80°) and trunk upright.

*Gastric Sensitivity to Intragastric Bag Distension*

After a 30-min adaptation period, minimal distending pressure (MDP) was first determined by increasing the intrabag pressure by 1 mm Hg every 3 min until a volume of >30 ml was reached. Gastric perception was examined with bag distension using a barostat device [4, 5]. Isobaric distensions were performed in stepwise increments of 2 mm Hg starting from MDP and each lasting 2 min, while the corresponding intragastric volume was recorded continuously. Subjects were instructed to score feelings in the upper abdomen at the end of every distending step by using a graphic rating scale that combined verbal descriptors: 0, no perception; 1, weak/vague; 2, weak but significant; 3, moderate/vague; 4, moderate but significant; 5, severe discomfort; and 6, unbearable pain. The endpoint of each sequence of distensions was established at an intrabag volume of 750 ml or when the subject reported unbearable pain (score 6).

*Gastric Accommodation*

For gastric accommodation, the bag pressure level was set at MDP + 2 mm Hg. After 20 min, the subject was requested to drink 200 ml of a liquid meal (Ensure-H®; 1.5 kcal/ml, 31.5% fat, 54.5% carbohydrate, 14.0% protein; Abbott Japan, Tokyo, Japan) through a straw over the course of 5 min. Recording of dyspepsia symptoms was continued for 60 min after the meal. Gastric tone before and after administration of the meal was measured by calculating the mean balloon volume for consecutive 1-min intervals. Maximal gastric volume recorded after drinking was determined as the 'peak accommodation volume'. The difference between the peak accommodation volume and the preprandial averaged volume during 20 min was also calculated as the meal-induced relaxation volume. Postprandial averaged gastric volume calculated over 60 min was investigated as an 'averaged accommodation volume'. The difference between the averaged accommodation volume and the preprandial averaged volume was also examined as an averaged meal-induced relaxation volume.

*Nutrient Drinking Test*

The drinking test was conducted on another day, at a maximum of 4 weeks from the barostat study. The study was performed after fasting for more than 6 h. Researchers served subjects 15 ml of Ensure-H® every 1 min, and subjects were ordered to continue drinking the liquid meal at a rate of 15 ml/min through a straw and to score satiation on a scale graded 0–5 at 5-min intervals. Participants were instructed to cease drinking when their score reached 5 (maximal satiation) or they had ingested 1,500 ml. Other dyspeptic symptoms, such as a bloated

sensation, pain, nausea and reflux, were also scored on a scale graded 0 (none) to 3 (severe) every 5 min.

*Reproducibility of the Drinking Test*

Seventeen subjects participated in a second drinking test to evaluate the reproducibility of this method. The second examination was conducted 8 weeks later using the same method as the first.

*Effects of Mosapride on the Drinking Test*

The effect of mosapride citrate (Gasmotin®; Dainippon-Sumitomo Pharmaceutical, Osaka, Japan) on the drinking test was determined using a randomized, double-blind, placebo-controlled, crossover design. After the first drinking test, 10 volunteers were randomly placed into two groups and received either mosapride (5 mg, t.i.d.) or placebo (5 mg, t.i.d.) as the first medication for a period of 2 weeks. The second drinking test was performed on the last day of the first medication. After a 2-week washout period, subjects in each group were changed to the other treatment regimen for another 2 weeks, with a third drinking test performed on the last day of the second medication. Lactose was used as a placebo; a mosapride tablet ground into powder and the placebo were provided in identical capsules.

*Statistical Analysis*

Data are expressed as means ± standard error of the mean with 95% CI. Statistical evaluation was performed using Pearson's correlation analysis and a paired t test. $p < 0.05$ was considered statistically significant. Analyses were performed using Office Excel 2003 (Microsoft, Redmond, Wash., USA) and StatView (SAS Institute, Cary, N.C., USA) software.

## Results

*Perception of Gastric Distention*

The mean MDP for all subjects was 6.6 ± 0.4 mm Hg (CI: 5.8–7.4). Three subjects did not score 5 or 6 at a bag volume of 750 ml. With increasing gastric pressure, increasing scores of the upper abdominal sensation were generated (fig. 1). First perception (score 1, n = 18), severe discomfort (score 5, n = 15) and unbearable pain (score 6, n = 15) were reported at distended pressures of 11.7 ± 1.0 mm Hg (9.6–13.8), 17.7 ± 0.8 mm Hg (15.9–19.4) and 20.3 ± 0.8 mm Hg (18.7–22.0), respectively, over MDP. The corresponding intragastric balloon volumes were 280 ± 37 ml (202–359), 544 ± 24 ml (493–594) and 607 ± 19 ml (567–648), respectively. Mean gastric compliance was 46.5 ± 4.0 ml/mm Hg (37.9–55.0).

*Peak Gastric Volume as Evaluated by a Barostat*

To evaluate postprandial gastric volume, the mean preprandial intragastric balloon volume at MDP +2 mm Hg was 172 ± 15 ml (139–206). In 14 of 18 subjects, ingestion of the nutrient induced an increment in the balloon volume located in the proximal stomach, indicating rapid relaxation, namely accommodation (adaptive relaxation). This phenomenon was not observed in 2 subjects for whom postprandial gastric volume was less than the baseline gastric volume (negative accommodation); these subjects were excluded from the test for these technical reasons [18]. In addition, 2 subjects did not tolerate drinking the nutrient and experienced vomiting reflux. We therefore excluded data from these 4 participants when analyzing the accommodation values.

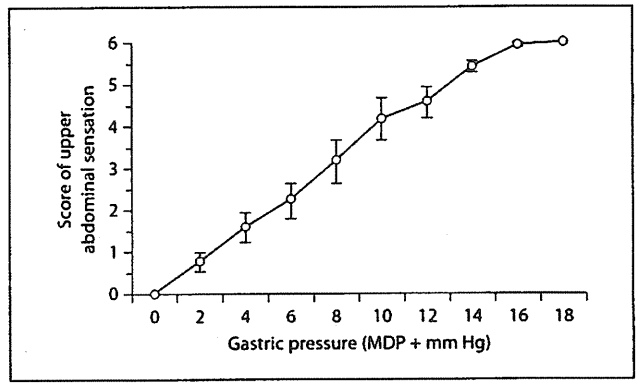


**Fig. 1.** Score of upper abdominal sensation during gastric distension by a barostat device. Isobaric distensions were performed in stepwise increments of 2 mm Hg starting from MDP and each lasting 2 min. The bar represents the standard error for the respective mean score.

Two minutes after drinking, the balloon volume was significantly greater than the mean preprandial volume. The peak volume (mean: 330 ± 28 ml, 270–390) was achieved 9 min after drinking and remained significantly elevated until 60 min postprandially.

Peak accommodation volume was 452 ± 27 ml (395–510). Meal-induced relaxation volume was 279 ± 27 ml (222–337). One hour after the meal, the mean intrabag volume was 291 ± 3 ml (225–357), corresponding to an increase of 230 ± 23 ml (180–280).

*Drinking Test*

A highly significant correlation existed between satiety scores and amount of drink ingested ($r = 0.80$, $p < 0.0001$). The volumes inducing first perception and maximum satiety were distributed from 75 to 300 ml (mean: 133 ± 14 ml, CI: 103–164), and from 345 to 1,500 ml (mean: 731 ± 72 ml, 581–883), respectively. All subjects complained of a bloated sensation, and the threshold volume inducing the first bloated sensation was 75–1,275 ml (mean: 283 ± 66

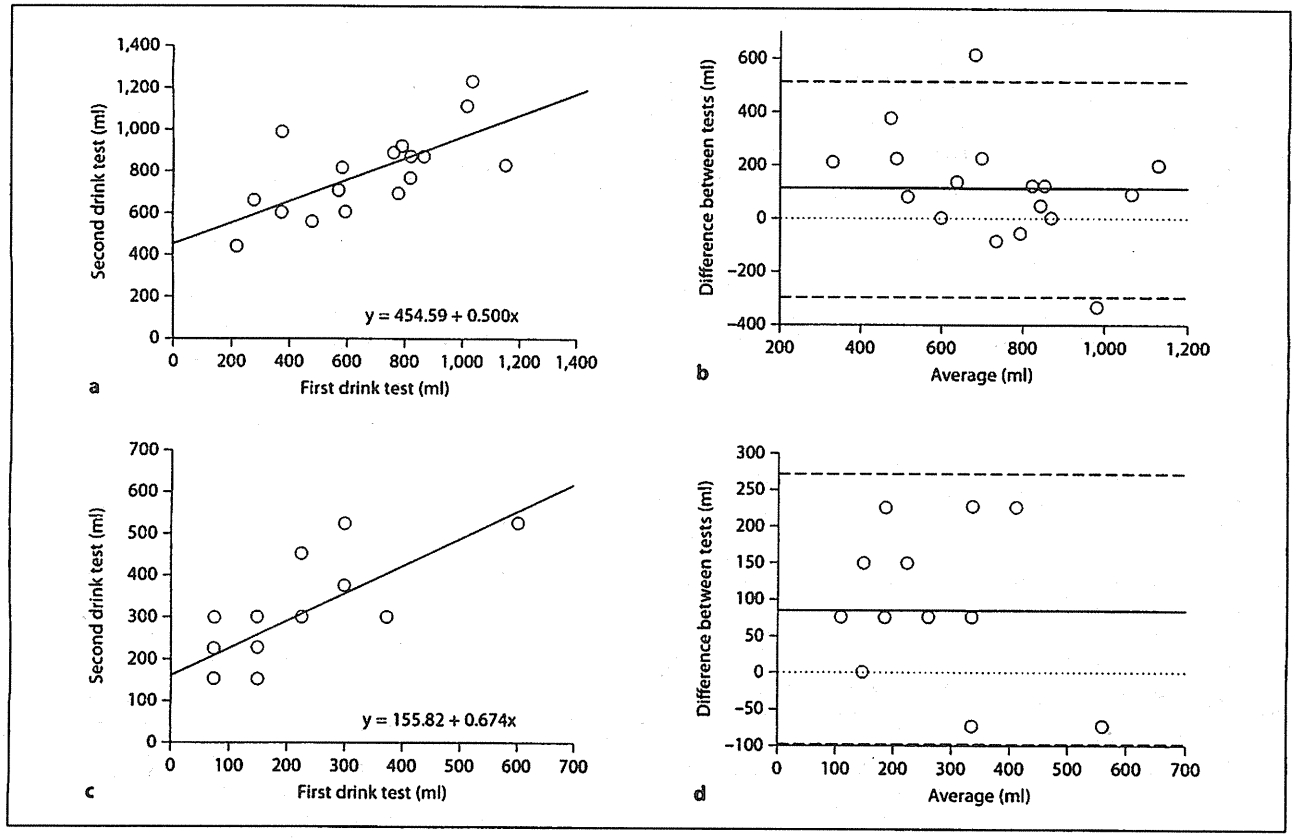


**Fig. 2.** Reproducibility of the slow nutrient drinking test. A good correlation for the maximal satiety volume (**a**: r = 0.67, p = 0.003) and the threshold volume inducing a bloated feeling (**c**: r = 0.75, p = 0.0005) was found between the first and the second drinking test, respectively. Bland-Altman plot (**b**: maximal satiety volume; **d**: threshold volume inducing a bloated feeling) showing the relationship between the mean of the two drinking tests and the difference between both. Horizontal lines indicate the levels of the mean and 95% limits of agreement [**b**: 115 (–284, 513); **d**: 88 (–94, 270)].

ml, 144–423). However, other dyspeptic symptoms were not necessarily reported by all subjects. Rates of nausea, pain and reflux were 83.3, 16.7 and 55.6%, respectively.

*Reproducibility*

As shown in figure 2, comparing the results obtained in the first and second drinking tests, good reproducibility was demonstrated for both the maximal satiety volume and the threshold volume inducing a bloated feeling. When correlation coefficients were calculated, the former was 0.67 (p = 0.003) and the latter was 0.75 (p = 0.0005).

*Correlations among Parameters Evaluated by the Barostat Study and the Drinking Test*

Neither pressure nor volume inducing first perception (score 1) or unbearable pain (score 6) in the barostat studies correlated with any parameters recorded during the drinking tests (table 1). However, pressure inducing severe discomfort (score 5) correlated positively with maximum satiety volume in the drinking test (r = 0.60, p = 0.02; fig. 3).

Accommodation volume (postprandial peak gastric volume) in the barostat study showed a significant correlation (r = 0.59, p = 0.03) with a threshold volume to induce bloating in the drinking test (fig. 4), but no correlation (r = 0.38, p = 0.18) with satiation volume. No other correlation was observed among the parameters provided by the drinking test and those by the barostat studies (table 1).

*Effects of Mosapride on the Drinking Test*

The maximum satiety volume was 524 ± 71 ml (364–683) in the pretreatment test, 783 ± 69 ml (628–938) after

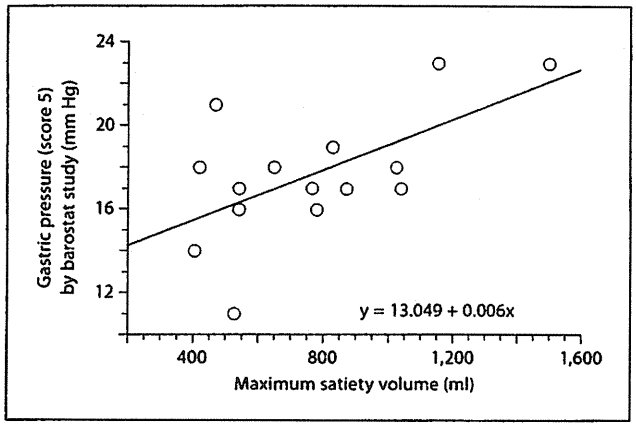


**Fig. 3.** Correlation between severe discomfort gastric pressure and maximum satiety volume. Pressure inducing severe discomfort (score 5) in barostat studies correlated positively with maximum satiety volume in the drinking test ($r = 0.60$, $p = 0.02$).

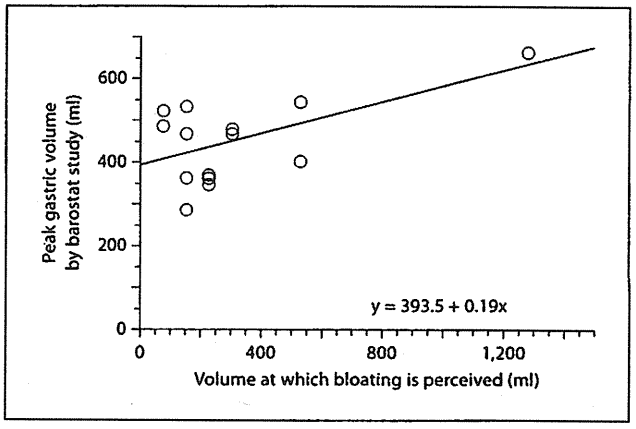


**Fig. 4.** Correlation between peak gastric volume and threshold volume inducing a significant bloated feeling. A significant correlation was identified between barostat peak gastric volume and drinking volume resulting in a significant bloated feeling ($r = 0.59$, $p = 0.03$).

**Table 1.** Correlations among parameters evaluated by the barostat study and the drinking test

| Barostat | Nutrient drink test | | | | | | | | | | | | | | |
|---|---|---|---|---|---|---|---|---|---|---|---|---|---|---|---|
| | maximal satiety (n =18) | | | bloated sensation (n = 18) | | | nausea (n = 15) | | | pain (n = 3) | | | reflux (n = 10) | | |
| | n | r | p | n | r | p | n | r | p | n | r | p | n | r | p |
| Score 1 pressure | 18 | 0.35 | 0.16 | 18 | 0.39 | 0.11 | 15 | 0.07 | 0.81 | 3 | 0.35 | 0.77 | 10 | 0.07 | 0.84 |
| Score 1 volume | | 0.32 | 0.19 | | 0.45 | 0.06 | | 0.32 | 0.24 | | 0.30 | 0.81 | | 0.55 | 0.10 |
| Score 5 pressure | 15 | 0.60 | 0.02* | 15 | 0.28 | 0.31 | 12 | 0.35 | 0.26 | 1 | 1.00 | – | 7 | 0.76 | 0.05 |
| Score 5 volume | | 0.28 | 0.31 | | 0.29 | 0.30 | | 0.16 | 0.63 | | 1.00 | – | | 0.18 | 0.71 |
| Score 6 pressure | 15 | 0.43 | 0.11 | 15 | 0.08 | 0.77 | 12 | 0.15 | 0.63 | 1 | 1.00 | – | 7 | 0.32 | 0.48 |
| Score 6 volume | | 0.12 | 0.66 | | 0.14 | 0.63 | | 0.33 | 0.30 | | 1.00 | – | | 0.65 | 0.11 |
| Accommodation | 14 | 0.38 | 0.18 | 14 | 0.59 | 0.03* | 11 | 0.21 | 0.53 | 3 | 1.00 | 0.45 | 6 | 0.13 | 0.80 |

* $p < 0.05$.

the placebo and 842 ± 92 ml (634–1,048) after mosapride. Respective volumes after the placebo or mosapride significantly increased in comparison with those in the pretreatment. However, no significant difference was observed between after the placebo and after mosapride. In contrast, volumes inducing the first bloated sensation were 233 ± 52 ml (115–350), 300 ± 65 ml (153–448) and 389 ± 92 ml (180–597), respectively. A trend toward an increase was observed in volumes after mosapride in comparison with those after the placebo, but this was not statistically significant ($p = 0.07$).

## Discussion

In the present study, only male adults were recruited to avoid the effects of any gender difference [19]. Novel findings of the present study were as follows: (1) the threshold volume inducing mild but significant bloating in the slow nutrient drinking test correlated with gastric peak accommodation volume as determined by the barostat method in Japanese men; and (2) the pressure to induce severe discomfort in the barostat method correlated positively with maximum satiety volume in the drinking test.

The optimal time frame for evaluation of meal-induced accommodation has not been established [4, 18]. We analyzed both peak and averaged value of postprandial proximal gastric volume. Peak value reflected a bloated feeling well, while the averaged value did not. In fact, a similar negative result was observed in normal volunteers in the previous study [4]. Changes in the proximal gastric volume after achieving peak accommodation showed various patterns over 1 h. In addition, our preliminary findings were that the time to reach peak volume reflected the initial changing point of the gastric emptying pattern, as determined by simultaneously monitoring the proximal volume by using a barostat and emptying by the breath test [20], suggesting that the time to reach peak volume reflects achieving the adaptive relaxation reflex. Moreover, the evaluation of gastric volume by magnetic resonance imaging, single-photon emission computed tomography (SPECT) and US measures peak value [21]. Taken together, peak postprandial gastric volume might more intimately reflect the physiological adaptive reflex reaction, namely the accommodation phenomenon.

The correlation between the maximum satiety drinking volume and gastric (accommodation) volume as measured by the barostat study is controversial [21]. Several factors might be responsible for inconsistencies. No standardization in drinking test methodologies is one serious issue that can result in different findings. Differences in drinking rates may underlie some discrepancies since a slower drinking rate may be required for full accommodation reflex [4, 22]. Difficulties in performing both tests simultaneously limit the validation of novel methods compared to the standard. Using scintigraphy, a radioactive nutrient drinking test showed good correlations among proximal gastric volume, satiety scores and maximum satiety volume [23]. However, when measuring gastric volume with SPECT, no correlation was observed between gastric volume and maximum satiety volume for a drinking test at a rate of 30 ml/min (0.95 kcal/ml) [10].

We used a slow drinking rate (15 ml/min) with a high caloric density (1.5 kcal/ml). Caloric density may influence the results, although no difference in the satiety score was seen by the Leuven group when increasing the caloric density in the range of 1.5–2 kcal/ml for the same volume of meal ingested [5]. The current study was performed using a method similar to that reported by Tack et al. [4] in which a good correlation between the maximum satiety drinking volume and the averaged postprandial gastric volume, as determined by the barostat study, was demonstrated in FD patients, but not in normal volunteers. In the present study, no significant correlation was observed in volunteers between the maximum satiety drinking volume and the peak, nor averaged postprandial gastric volume. Further studies in FD patients using methods similar to the present study are thus warranted. In addition, the importance of the novel finding that a threshold volume inducing mild bloating in the slow nutrient drinking test might be an alternative parameter of gastric accommodation volume as determined by the barostat method should be confirmed by repeating the same experiment or sampling more data.

The maximum satiety volume in the drinking test correlated positively with the pressure to induce severe discomfort (score 5), but not unbearable pain (score 6), in a barostat study. A threshold of pain sensation from mild to unbearable against mechanical distension stimulus can be measured by a barostat. Satiety might be induced not only by mechanical gastric distension, but also by chemical stimulus under slow-drinking conditions [21]. Only 3 of 18 subjects (16.6%) reported pain at the maximum satiety volume in this study. Therefore, the satiety drinking test might be unable to estimate the intragastric pressure to induce unbearable pain.

The endpoint of the slow nutrient drinking test is sensitive to pharmacological manipulations of gastric motor function [12]; therefore, in a preliminary study, we investigated the effects of certain prokinetics on the present drinking test. In the current study, we chose mosapride citrate for the following reasons. First, mosapride citrate accelerates gastric motility and emptying [24]. Second, this compound is widely accepted as an effective drug against dyspeptic symptoms in Asian countries [15]. Third, a large clinical trial in Japan demonstrated that this drug improves gastric stasis and epigastric pain in FD patients [16]. Fourth, pretreatment with 5-HT4 receptor agonists cisapride or tegaserod significantly enhances postprandial fundic accommodation, indicating that 5-HT4 receptor activation may enhance gastric accommodation reflex in humans [25–28].

We therefore hypothesized that mosapride might enhance accommodation. Our double-blind trial of administration of this drug to normal volunteers proved that this drug tended to increase the threshold volume resulting in a bloated sensation in the drinking test. Although reproducibility of the present drinking test has been demonstrated and is in agreement with recent findings [12], a significant increase in the volume was observed after 2 weeks of administration of mosapride and placebo.

Mearin et al. [29] demonstrated several significant changes in gastric motor function, such as an increase in gastric phase III number and in the postprandial antral motility index accompanied by symptom relief after 8 weeks with placebo in FD patients, suggesting that a placebo might modulate certain gastric functions demonstrated in the present study. In addition, the carryover (period-treatment) effect of subjective feelings, which is among the disadvantages of crossover designs, might affect the results of the placebo administration [30] because the endpoint (volumes inducing the first bloated sensation) of the present study was not only objective, but also subjective.

In a recent Japanese study, mosapride significantly enhanced gastric accommodation as determined by US in 14 normal volunteers in a parallel group design [17]. We observed a trend of increasing effect of the drug on the drinking volume to induce a bloated sensation, which may correspond to accommodation, although the dose and duration of prescription of mosapride or placebo in the present study were similar. To confirm the significant effect of the drug in the present drinking study, further investigation with a larger number of subjects (to avoid a beta-error due to the small sample size) and a parallel group design might be warranted.

In conclusion, our noninvasive drinking test may be useful for evaluating the threshold to induce severe discomfort and accommodation volume in volunteers.


## Acknowledgment

We thank Professor Emeritus Shinichi Kakumu for his suggestions and encouragement throughout this study.

## Disclosure Statement

This work was supported in part by a Grant-in-Aid for Scientific Research from the Aichi Medical University Alumni Association. There are no potential conflicts of interest for any of the authors in relation to the contents of the article.


## References


1 Tack J, Talley NJ, Camilleri, Holtmann MG, Hu P, Malagelada JR, Stanghellini V: Functional gastroduodenal disorders. Gastroenterology 2006;130:1466–1479.

2 Talley NJ, Choung RS: Whither dyspepsia? A historical perspective of functional dyspepsia, and concepts of pathogenesis and therapy in 2009. J Gastroenterol Hepatol 2009; 24(suppl 3):S20–S28.

3 Mimidis K, Tack J: Pathogenesis of dyspepsia. Dig Dis 2008;26:194–202.

4 Tack J, Piessevaux H, Coulie B, Caenepeel P, Janssens J: Role of impaired gastric accommodation to a meal in functional dyspepsia. Gastroenterology 1998;115:1346–1352.

5 Tack J, Caenepeel P, Piessevaux H, Cuomo R, Janssens J: Assessment of meal induced gastric accommodation by a satiety drinking test in health and in severe functional dyspepsia. Gut 2003;52:1271–1277.

6 Boeckxstaens GE, Hirsch DP, Elzen BDJ, Heisterkamp SH, Tytgat GNJ: Impaired drinking capacity in patients with functional dyspepsia: relationship with proximal stomach function. Gastroenterology 2001; 121:1054–1063.

7 Zwart IM, Haans JJL, Verbeek P, Eilers PHC, Roos A, Masclee AAM: Gastric accommodation and motility are influenced by the barostat device: assessment with magnetic resonance imaging. Am J Physiol Gastrointest Liver Physiol 2007;292:G208–G214.

8 Jones MP, Hoffman S, Shah D, Patel K, Ebert CC: The water load test: observations from healthy controls and patients with functional dyspepsia. Am J Physiol Gastrointest Liver Physiol 2003;284:G896–G904.

9 Hjelland IE, Ofstad AP, Narvestad JK, Berstad A, Hausken T: Drink tests in functional dyspepsia: which drink is best? Scand J Gastroenterol 2004;39:933–937.

10 Gonenne J, Castillo EJ, Camilleri M, Burton D, Thomforde GM, Baxter KL, Zinsmeister AR: Does the nutrient drink test accurately predict postprandial gastric volume in health and community dyspepsia? Neurogastroenterol Motil 2005;17:44–50.

11 Kato M, Nishida U, Nishida M, Hata T, Asaka R, Haneda M, Yamamoto K, Imai A, Yoshida T, Ono S, Shimizu Y, Asaka M: Pathophysiological classification of functional dyspepsia using a novel drinking-ultrasonography test. Digestion 2010;82:162–166.

12 Kindt S, Coulie B, Wajs E, Janssens J, Tack J: Reproducibility and symptomatic predictors of a slow nutrient drinking test in health and in functional dyspepsia. Neurogastroenterol Motil 2008;20:320–329.

13 Jones MP: Satiety testing: ready for the clinic? World J Gastroenterol 2008;14:5371–5376.

14 Curran MP, Robinson DM: Mosapride in gastrointestinal disorders. Drugs 2008;68: 981–991.

15 Kinoshita Y, Hashimoto T, Kawamura A, Yuki M, Amano K, Sato H, Adachi K, Sato S, Oshima N, Takashima T, Kitajima N, Abe K, Suetsugu H: Effects of famotidine, mosapride and tandospirone for treatment of functional dyspepsia. Aliment Pharmacol Ther 2005;21(suppl 2):37–41.

16 Hongo M: Initial approach and pharmacotherapy for functional dypepsia – a large clinical trial in Japan. Gastroenterology 2006;130:A-506.

17 Kusunoki H, Haruma K, Hata J, Kamada T, Ishii M, Yamashita N, Inoue K, Imamura H, Manabe N, Shiotani A: Efficacy of mosapride citrate in proximal gastric accommodation and gastrointestinal motility in healthy volunteers: a double-blind placebo-controlled ultrasonographic study. J Gastroenterol 2010;45:228–234.

18 Tutuian R, Vos R, Karamanolis G, Tack J: An audit of technical pitfalls of gastric barostat testing in dyspepsia. Neurogastroenterol Motil 2008;20:113–118.

19 Chial HJ, Camilleri C, Delgado-Aros S, Burton D, Thomforde G, Ferber I, Camilleri M: A nutrient drink test to assess maximum tolerated volume and postprandial symptoms: effects of gender, body mass index and age in health. Neurogastroenterol Motil 2002;14: 249–253.

20 Konagaya T, Iida A, Funaki Y, Imamura H, Tokudome K, Kaneko H, Kakumu S: Implication in pattern of continuous 13C breath testing for gastric emptying by simultaneous comparison with gastric fundic accommodation curve by a barostat device. Gastroenterology 2007;132:A-372.
21 Mimidis K: Drinking tests in functional dyspepsia: what do they really measure? Neurogastroenterol Motil 2007;19:947–950.
22 Tack J: Drink tests in functional dyspepsia. Gastroenterology 2002;122:2093–2094.
23 Piessevaux H, Tack J, Walrand S, Pauwels S, Geubel A: Intragastric distribution of a standardized meal in health and functional dyspepsia: correlation with specific symptoms. Neurogastroenterol Motil 2003;15:447–455.
24 De Maeyer JH, Lefebvre RA, Schuurkes JAJ: 5-HT4 receptor agonists: similar but not the same. Neurogastroenterol Motil 2008;20: 99–112.
25 Tack J, Vos R, Janssens J, Salter J, Jauffret S, Vandeplassche G: Influence of tegaserod on proximal gastric tone and on the perception of gastric distension. Aliment Pharmacol Ther 2003;18:1031–1037.
26 Tack J, Broeckaert D, Coulie B, Janssens J: The influence of cisapride on gastric tone and the perception of gastric distension. Aliment Pharmacol Ther 1998;12:761–766.
27 Degen L, Matzinger D, Merz M, Appel-Dingemanse S, Osborne S, Luchinger S, Bertold R, Maecke H, Beglinger C: Tegaserod, a 5-HT4 receptor partial agonist, accelerates gastric emptying and gastrointestinal transit in healthy male subjects. Aliment Pharmacol Ther 2001;15:1745–1751.
28 Muller-Lissner SA, Fumagalli I, Bardhan KD, Pace F, Pecher E,Nault B, Rüegg P: Tegaserod, a 5-HT4 receptor partial agonist, relieves symptoms in irritable bowel syndrome patients with abdominal pain, bloating and constipation. Aliment Pharmacol Ther 2001; 15:1655–1666.
29 Mearin F, Balboa A, Zárate N, Cucala M, Malagelada JR: Placebo in functional dyspepsia: symptomatic, gastrointestinal motor, and gastric sensorial responses. Am J Gastroenterol 1999;94:116–125.
30 Hills M, Armitage P: The two-period cross-over clinical trial. Br J Clin Pharmacol 2004; 58:S703–S716.

Hepatology Research

*Hepatology Research* 2011; 41: 921–924 doi: 10.1111/j.1872-034X.2011.00895.x

*Review Article*

# Liver stiffness measurement using transient elastography and hepatocellular carcinoma

Haruhisa Nakao and Masashi Yoneda

*Division of Gastroenterology, Department of Internal Medicine, Aichi Medical University, Nagakute, Aichi, Japan*

Liver fibrosis has been gaining noticeable attention because it may lead to end-stage liver cirrhosis and ultimately to hepatocellular carcinoma. Thus, a precise estimation of the degree of liver fibrosis is crucial for predicting prognosis and deciding management of patients with chronic liver diseases. Many non-invasive approaches for the evaluation of liver fibrosis have been developed. Among these procedures, transient elastography has recently drawn great attention. Transient elastography has been reported to be well correlated with the degree of liver fibrosis by many investigators and various institutions. Since the degree of liver fibrosis is considered as a strong predictor of risk for hepatocellular carcinoma development, several trials have been performed to verify the usefulness of measurement of liver stiffness to predict the emergence of hepatocellular carcinoma. From these studies, transient elastography seems to be a promising procedure to predict the risk of hepatocellular carcinoma; however, further cohorts with long-term monitoring of liver stiffness are needed to confirm the usefulness of this method.

**Key words:** chronic liver disease, hepatocellular carcinoma, liver cirrhosis, liver fibrosis, transient elastography

## INTRODUCTION

LIVER FIBROSIS IS a common pathway for liver injury and results in hepatocellular dysfunction, expansion of extracellular matrix with distortion of hepatic architecture, portal hypertension, and, finally, cirrhosis, which may develop hepatocellular carcinoma (HCC).[1,2] It is known that liver fibrosis is the strongest prognostic indicator of chronic liver diseases, which is evaluated by liver biopsy.[3–5] Therefore, a precise estimation of the presence and the degree of liver fibrosis is indispensable for predicting prognosis and planning treatment of patients with chronic liver diseases.[6] Liver biopsy is considered to be the gold standard for the assessment of the grades of liver fibrosis. However, liver biopsy is an invasive method, which is associated with a risk of serious complications, and carries a risk of mortality ranging from 1 in 1000 to 1 in 10 000.[7,8] In addition, the accuracy of liver biopsy is limited as a result of inter-observer variability and sampling errors.[8,9] The limitation of liver biopsy led to considerable studies of non-invasive approaches for the assessment of liver fibrosis to reduce the need for biopsy. A great variety of non-invasive methods for the evaluation of liver fibrosis have been developed. The non-invasive methods include numerous hematologic and biochemical tests, complex algorithms based on maker panels, radiologic imaging such as magnetic resonance elastography (MRE) and single photon emission computed tomography (SPECT), and transient elastography.[6,10,11]

*Correspondence: Dr Haruhisa Nakao, Division of Gastroenterology, Department of Internal Medicine, Aichi Medical University, 21 Karimata Yazako, Nagakute, Aichi 480-1195, Japan. Email: hnakao@aichi-med-u.ac.jp*
*Received 10 August 2011; revision 16 August 2011; accepted 22 August 2011.*

## TRANSIENT ELASTOGRAPHY

IN THE LAST decade, an increasing number of studies have evaluated transient elastography (FibreScan; Echosens, Paris, France) for the estimation of liver fibrosis in various liver diseases, such as viral hepatitis, alcoholic liver disease, non-alcoholic steatohepatitis (NASH), primary biliary cirrhosis (PBC), primary sclerosing cholangitis (PSC), or hemochromatosis, and, as a result, liver stiffness estimated by using transient elastography was correlated with the degree of hepatic fibrosis.[12–16] Since a great number of investigations have proved that transient elastography is a rapid, non-invasive, and reproducible method to assess liver fibrosis by measuring liver stiffness, transient elastography

has been accepted as a promising non-invasive marker to assess liver fibrosis stage.[17–20] Transient elastography is performed with an ultrasound transducer probe mounted on a vibrator. Vibrations transmitted from the vibrator toward the tissue produce elastic share waves that propagate throughout the liver. The probe also emits a pulse-echo ultrasound wave, which is used to measure the velocity of the share wave. The velocity of the share wave is directly related to liver stiffness. The harder the tissue, the faster the share wave propagates. Liver stiffness values are expressed in kilopascals (Kpa) and range from 2.4 to 75 kPa.[21] Roulot *et al.* showed that the mean value of liver stiffness in healthy subjects was 5.5 ± 1.59 kPa with the range from 3.3 to 7.8 kPa in women and from 3.8 to 8.0 kPa in men.[22] Sirli *et al.* reported that the mean values of liver stiffness in individuals without known hepatic pathology were 4.8 ± 1.3 kPa, ranging from 2.3 to 8.8 kPa, and that age did not modify the liver stiffness.[23]

## ESTIMATION OF LIVER FIBROSIS BY TRANSIENT ELASTOGRAPHY

THE PRESENCE OF significant liver fibrosis (F2 or more stage according to the METAVIR scoring system) is considered evidence of a progressive liver disease. Several studies have shown that cut-off values for a diagnosis of fibrosis F2 (moderate fibrosis) ranged from 7.1 to 8.8 kPa and cut-off values for a diagnosis F3 (severe fibrosis) ranged from 9.5 to 12.5 kPa.[12,20,24] Although transient elastography is valued for the estimation of significant liver fibrosis, it performed best for the differentiation of cirrhosis (F4) and no cirrhosis (F0/1/2/3). While previous studies demonstrated that cut-off values for the diagnosis of cirrhosis ranged from 12.5 to 17.6 kPa,[12,25,26] the liver stiffness value of 12.5 kPa was frequently used as a cut-off value for diagnosis of cirrhosis. In addition, liver stiffness values in cirrhotic patients widely ranged from 12.5 to 75 kPa.[12] Liver stiffness values in patients with cirrhosis increased as the liver disease progressed. Foucher *et al.* established the cut-off value for complications of cirrhosis with a negative predictive value of more than 90%. These cut-off values were 27.5 kPa for the presence of esophageal varices stage 2 or 3, 37.5 kPa for cirrhosis Child score B or C, 49.1 kPa for a past history of ascites, 53.7 kPa for HCC, and 62.7 kPa for esophageal bleeding.[12] Transient elastography might be useful not only for the diagnosis of cirrhosis but also the follow up and management of patients with cirrhosis. However, it is important to note that transient elastography is not suitable for an estimation of the staging of liver fibrosis in patients with hepatitis exacerbation or acute hepatitis because necroinflammatory activity influences transient elastography values and transient elastography might overestimate the stage of liver fibrosis during alanine aminotransferase flare.[18,19,27] In addition, liver stiffness values measured by transient elastography are increased in patients with cholestasis or liver congestion, independent of the degree of fibrosis.[28,29] Moreover, transient elastography is unable to be performed on patients with ascites, as well as on patients with narrow intercostal spaces or severe obesity.

## PREDICTION OF HCC DEVELOPMENT BY TRANSIENT ELASTOGRAPHY

THE DEGREE OF liver fibrosis has been reported to be the strongest predictor of risk of HCC development.[5] Thus, the estimation of the risk for HCC development is essential in the management of patients with chronic liver diseases. Masuzaki *et al.* revealed that liver stiffness measurement using transient elastography was strongly associated with the probability of the presence of HCC among patients with hepatitis C in a cross-section setting.[30] The usefulness of transient elastography for the estimation of predicting the risk of HCC development was also suggested in other cross-sectional setting studies, intended for patients with hepatitis B and C, and for patients with hepatitis C and alcoholic liver disease.[10,31] On the other hand, prospective cohort studies published previously, with respect to the association between liver stiffness measured by transient elastography and the risk of HCC development, consist of only two papers at present. The first large prospective cohort was intended for 866 patients with chronic hepatitis C, 77 of whom developed HCC during mean follow-up of 3 years, and demonstrated that the cumulative incidence of HCC increased with baseline liver stiffness values, ranging from 0.4% at 3 years in patients with liver stiffness values ≤ 10 kPa to 38.5% in patients with liver stiffness values >25 kPa.[32] Furthermore, it was found that liver stiffness measurement was the strongest predictor of HCC onset, with relative risks of 16.7, 20.0, 25.6, and 45.5 for liver stiffness measurement values of 10–15 kPa, 15–20 kPa, 20–25 kPa, and >25 kPa, respectively. Another prospective cohort suggested that a liver stiffness measurement of 10 kPa was associated with a significantly increased risk of subsequent HCC development and mortality in 528 patients with HBeAg-negative chronic hepatitis B.[33]

Recently, Akima *et al.*[34] examined the correlation between liver stiffness measurement using transient elastography and HCC presence in 157 patients with HBV or HCV, and, subsequently, investigated the significance of liver stiffness estimated by transient elastography at the start of observation, as a predictor of HCC development, on a prospective cohort of 106 patients without HCC, 10 of whom developed HCC during mean follow-up of 40.7 months. The values of liver stiffness were significantly higher in 41 patients with HCC (24.9 ± 19.5 kPa) than 116 patients without HCC (10.9 ± 11.0 kPa). Additionally, it was suggested that the diagnostic accuracy of liver stiffness for the presence of HCC, on the basis of respective area under the receiver operating characteristic curves (AUROCs), might be superior to age, platelet cell count, prothrombin activity, alpha-fetoprotein (AFP), and des-gammma-carboxy prothrombin (DCP). The cut-off value of liver stiffness for the presence of HCC, determined from the ROC curve, was 12.5 kPa, which was used for analysis of the relation between liver stiffness and HCC development in 116 patients without HCC at the beginning on a subsequent prospective cohort. The prospective cohort demonstrated that the mean value of liver stiffness in 10 patients with HCC development was 20.0 ± 10.5 kPa, significantly higher than in 96 patients without HCC development 9.9 ± 7.6 kPa. Moreover, multivariate analysis revealed that liver stiffness values ≥12.5 kPa, age ≥60, and serum total bilirubin ≥1.0 mg/dL were significantly correlated with development of HCC. In regard to different etiology for chronic liver diseases, it has been suggested that HBV patients seemed to have a higher risk of HCC presence than HCV patients, in cirrhotic liver at the same stiffness level, because of the difference between HBV and HCV in mechanisms of hepatocarcinogenesis.[31,35] Although the cut-off value of 10 kPa was used in the previous two prospective cohort studies, 12.5 kPa, which is generally accepted as a cut-off value for cirrhosis, was applied in the recent study by Akima *et al.* The optimal cut-off value of liver stiffness by transient elastography for the prediction of HCC development in different causes remains to be determined.

## CONCLUSIONS

THE MEASUREMENT OF liver stiffness using transient elastography might be useful to estimate the risk for HCC development in patients with chronic liver diseases. Further large cohorts with long-term monitoring of liver stiffness progression are needed to confirm the accuracy of liver stiffness measurement using transient elastography as an indicator of the risk of HCC development.

## REFERENCES

1 Lauer GM, Walker BD. Hepatitis C virus infection. *N Engl J Med* 2001; 5: 41–52.
2 Benvegnu L, Gios M, Boccato S, Alberti A. Natural history of compensated viral cirrhosis: a prospective study on the incidence and hierarchy of major complications. *Gut* 2004; 53: 744–9.
3 Strader DB, Wright T, Thomas DL, Seeff LB. Diagnosis, management, and treatment of hepatitis C. *Hepatology* 2004; 39: 1147–71.
4 Yano M, Kumada H, Kage M *et al.* The long-term pathological evolution of chronic hepatitis C. *Hepatology* 1996; 23: 1334–40.
5 Yoshida H, Shiratori Y, Moriyama M *et al.* Interferon therapy reduces the risk for hepatocellular carcinoma: national surveillance program of cirrhotic and noncirrhotic patients with chronic hepatitis C in Japan. IHIT Study Group. Inhibition of Hepatocarcinogenesis by Interferon Therapy. *Ann Intern Med* 1999; 3: 174–81.
6 Smith JO, Sterling RK. Systematic review: non-invasive methods of fibrosis analysis in chronic hepatitis C. *Aliment Pharmacol Ther* 2009; 15: 557–76.
7 Bravo AA, Sheth SG, Chopra S. Liver biopsy. *N Engl J Med* 2001; 15: 495–500.
8 Bedossa P, Dargere D, Paradis V. Sampling variability of liver fibrosis in chronic hepatitis C. *Hepatology* 2003; 38: 1449–57.
9 Abdi W, Millan JC, Mezey E. Sampling variability on percutaneous liver biopsy. *Arch Intern Med* 1979; 139: 667–9.
10 Nahon P, Thabut G, Ziol M *et al.* Liver stiffness measurement versus clinicians' prediction or both for the assessment of liver fibrosis in patients with chronic hepatitis C. *Am J Gastroenterol* 2006; 101: 2744–51.
11 Rouviere O, Yin M, Dresner MA *et al.* MR elastography of the liver: preliminary results. *Radiology* 2006; 240: 440–8.
12 Foucher J, Chanteloup E, Vergniol J *et al.* Diagnosis of cirrhosis by transient elastography (FibroScan): a prospective study. *Gut* 2006; 55: 403–8.
13 Ganne-Carrie N, Ziol M, de Ledinghen V *et al.* Accuracy of liver stiffness measurement for the diagnosis of cirrhosis in patients with chronic liver diseases. *Hepatology* 2006; 44: 1511–17.
14 Yoneda M, Yoneda M, Fujita K *et al.* Transient elastography in patients with non-alcoholic fatty liver disease (NAFLD). *Gut* 2007; 56: 1330–1.
15 Corpechot C, El Naggar A, Poujol-Robert A *et al.* Assessment of biliary fibrosis by transient elastography in patients with PBC and PSC. *Hepatology* 2006; 43: 1118–24.
16 Adhoute X, Foucher J, Laharie D *et al.* Diagnosis of liver fibrosis using FibroScan and other noninvasive methods in

patients with hemochromatosis: a prospective study. *Gastroenterol Clin Biol* 2008; 32: 180–7.
17 Sandrin L, Fourquet B, Hasquenoph JM *et al.* Transient elastography: a new noninvasive method for assessment of hepatic fibrosis. *Ultrasound Med Biol* 2003; 29: 1705–13.
18 Arena U, Vizzutti F, Abraldes JG *et al.* Reliability of transient elastography for the diagnosis of advanced fibrosis in chronic hepatitis C. *Gut* 2008; 57: 1288–93.
19 Fraquelli M, Rigamonti C, Casazza G *et al.* Reproducibility of transient elastography in the evaluation of liver fibrosis in patients with chronic liver disease. *Gut* 2007; 56: 968–73.
20 Castera L, Vergniol J, Foucher J *et al.* Prospective comparison of transient elastography, Fibrotest, APRI, and liver biopsy for the assessment of fibrosis in chronic hepatitis C. *Gastroenterology* 2005; 128: 343–50.
21 Castera L, Forns X, Alberti A. Non-invasive evaluation of liver fibrosis using transient elastography. *J Hepatol* 2008; 48: 835–47.
22 Roulot D, Czernichow S, Le Clesiau H *et al.* Liver stiffness values in apparently healthy subjects: influence of gender and metabolic syndrome. *J Hepatol* 2008; 48: 606–13.
23 Sirli R, Sporea I, Tudora A *et al.* Transient elastographic evaluation of subjects without known hepatic pathology: does age change the liver stiffness? *J Gastrointestin Liver Dis* 2009; 18: 57–60.
24 Ziol M, Handra-Luca A, Kettaneh A *et al.* Noninvasive assessment of liver fibrosis by measurement of stiffness in patients with chronic hepatitis C. *Hepatology* 2005; 41: 48–54.
25 Castera L. Liver stiffness and hepatocellular carcinoma: liaisons dangereuses? *Hepatology* 2009; 49: 1793–4.
26 Friedrich-Rust M, Ong MF, Martens S *et al.* Performance of transient elastography for the staging of liver fibrosis: a meta-analysis. *Gastroenterology* 2008; 134: 960–74.
27 Coco B, Oliveri F, Maina AM *et al.* Transient elastography: a new surrogate marker of liver fibrosis influenced by major changes of transaminases. *J Viral Hepat* 2007; 14: 360–9.
28 Millonig G, Reimann FM, Friedrich S *et al.* Extrahepatic cholestasis increases liver stiffness (FibroScan) irrespective of fibrosis. *Hepatology* 2008; 48: 1718–23.
29 Millonig G, Friedrich S, Adolf S *et al.* Liver stiffness is directly influenced by central venous pressure. *J Hepatol* 2010; 52: 206–10.
30 Masuzaki R, Tateishi R, Yoshida H *et al.* Risk assessment of hepatocellular carcinoma in chronic hepatitis C patients by transient elastography. *J Clin Gastroenterol* 2008; 42: 839–43.
31 Kuo YH, Lu SN, Hung CH *et al.* Liver stiffness measurement in the risk assesment of hepatocellular carcinoma for patients with chronic hepatitis. *Hepatol Int* 2010; 4: 700–6.
32 Masuzaki R, Tateishi R, Yoshida H *et al.* Prospective risk assessment for hepatocellular carcinoma development in patients with chronic hepatitis C by transient elastography. *Hepatology* 2009; 49: 1954–61.
33 Fung J, Lai CL, Seto WK *et al.* Prognostic significance of liver stiffness for hepatocellular carcinoma and mortality in HBeAg-negative chronic hepatitis B. *J Viral Hepat* 2010; 2010 July 26 (Epub ahead of print); doi:10.1111/j.1365-2893.2010.01355.x.
34 Akima T, Tamada M, Hiraishi H. Liver stiffness measured by transient elastography is a predictor of hepatocellular carcinoma development in viral hepatitis. *Hepatol Res* 2011; 41: 965–70 (this issue).
35 Szabo E, Paska C, Kaposi-Novak P *et al.* Similarities and differences in hepatitis B and C virus induced hepatocarcinogenesis. *Pathol Oncol Res* 2004; 10: 5–11.

EBM-1105-RM-173

# Original Research

# Preventive effect of urinary trypsin inhibitor on the development of liver fibrosis in mice

**Toru Kono[1], Yurino Kashiwade[1], Toshiyuki Asama[1], Naoyuki Chisato[1], Yoshiaki Ebisawa[1], Masashi Yoneda[2] and Shinichi Kasai[1]**

[1]Division of Gastroenterologic and General Surgery, Department of Surgery, Asahikawa Medical University, Asahikawa, 2-1 Midorigaoka-Higashi, Hokkaido 078-8510; [2]Division of Gastroenterology, Department of Internal Medicine, School of Medicine, Aichi Medical University, Aichi, Japan

Corresponding author: Toru Kono. Email: kono@asahikawa-med.ac.jp

## Abstract

**Urinary trypsin inhibitor (UTI) is a serine protease inhibitor produced in the liver that inhibits the production and activation of various cytokines, notably transforming growth factor-β (TGF-β), which are associated with the progression of liver fibrosis. However, the various roles of endogenous UTI in liver fibrosis have not been examined. This study, therefore, examined the long-term effects of UTI deficiency during both steady-state conditions and thioacetamide (TA)-induced liver fibrosis. Furthermore, the effects of continuous exogenous UTI administration were examined. Analyses of liver fibrosis marker, hyaluronic acid (HA), TGF-β concentrations and histological findings at 30 weeks of age showed that homozygous UTI-knockout (KO) mice had higher HA and TGF-β concentrations than did heterozygous UTI-KO mice and wild-type mice, although there was no histological evidence of liver fibrosis in these mice. TA treatment for 20 weeks also resulted in greater HA and TGF-β levels in homozygous mice than in heterozygous and wild-type mice. Furthermore, homozygous mice had more severe liver fibrosis based on histological analyses. HA and TGF-β levels were lower in homozygous UTI-KO mice that were continuously administered UTI versus those given distilled water. These findings indicate that UTI deficiency leads to the production of HA and hepatic TGF-β and that administering exogenous UTI can ameliorate these changes. We conclude that endogenous UTI is produced in the liver to suppress the production and activation of TGF-β and that administering exogenous UTI may be therapeutically beneficial for preventing liver fibrosis.**

**Keywords:** urinary trypsin inhibitor, liver fibrosis, knockout mice, ulinastatin, TGF-β

*Experimental Biology and Medicine* 2011; 00: 1–8. DOI: 10.1258/ebm.2011.011173

## Introduction

Urinary trypsin inhibitor (UTI) is a serine protease inhibitor derived from the degradation of pre-α-/inter-α-trypsin inhibitors synthesized in the liver[1,2] in response to biological insults such as infection, surgery, trauma and inflammation.[3] This molecule is believed to serve as an intrinsic protective factor against biological insults. In Japan, patients with highly purified UTI, ulinastatin, has been clinically used in the treatment of circulatory shock and pancreatitis.[3,4] Research using the rat hepatic ischemia–reperfusion injury model found that exogenous administration of UTI significantly reduced liver damage.[5–8] However, little is known about the physiological significance of endogenous UTI for the liver, the organ that secretes this protease inhibitor.[1,2,9]

During hepatopathy induced by chronic inflammation (i.e. chronic hepatitis), damaged tissue is repaired by accumulated connective tissue, which causes the liver to ultimately become cirrhotic. As fibrosis is the most important factor in the onset of both carcinogenesis and hepatic failure, one important prophylactic and therapeutic strategy is to control the progression of hepatic fibrosis.[10,11] The progression of liver fibrosis has been shown to involve transforming growth factor-β (TGF-β), released from activated stellate cells, as well as plasmin, kallikrein and other liver serine proteases that activate stellate cells.[12–14]

Extensive investigation has been successfully revealing the intrinsic protective roles of UTI. One of the key actions of UTI identified to date is the suppression of the production of tumor necrosis factor-α, interleukin-1β and other inflammatory cytokines.[15,16] UTI has been recently reported to inhibit radiation-induced lung fibrosis by potentially suppressing TGF-β synthesis.[17] Other important effects of UTI include the inhibition of the release of

ISSN: 1535-3702

various proteases by stabilizing the lysosomal membrane.[18] Past research has identified that the target proteases of UTI include trypsin as well as serine proteases involved in the activation of TGF-$\beta$.[8,19-21]

These findings led us to hypothesize that UTI endogenously produced in the liver inhibits the development of liver fibrosis resulting from viral hepatitis and other causes by suppressing the production and activation of TGF-$\beta$.

In this study, we employed UTI-knockout (KO) mice to investigate the physiological significance of endogenously produced UTI in the prevention of liver fibrosis. We compared the differences among homozygous UTI-KO, heterozygous UTI-KO and wild-type mice in (1) age-related hepatic changes and (2) the development of liver fibrosis induced by the potent hepatotoxin thioacetamide (TA).[22]

## Materials and methods

### Animals

The UTI-KO mice used in this study (provided by the Research Center, Mochida Pharmaceutical Co, Ltd, Shizuoka, Japan) were generated by replacing exons 8 and 9 of the UTI gene with the neomycin-resistance gene.[23] Specifically, they were produced as follows: 129/Ola-derived embryonic stem (ES) cells were first transfected with the gene-targeting construct containing the neomycin-resistance gene, and gene-targeted ES cells were selected by screening for neomycin resistance. The selected ES cells were injected into host C57BL/6 blastocysts, and the blastocysts were transferred to the uterus of pseudo-pregnant ICR mice to produce chimeric offspring with a mosaic (black and white) coat color. Chimeras were then mated with C57BL/6 mice to yield white mice heterozygous for the gene KO (the coat color was the same as that for the original ES cell line), and these heterozygous mice were mated to finally produce homozygous KO mice. Western blot analysis was used to confirm the constitutive KO. The experimental protocols were approved by the Animal Care Committee of Asahikawa Medical University and were in accordance with the National Institute of Health's 'Guide for the Care and Use of Laboratory Animals'.

### Treatments and sample collection

Ten-week-old homozygous and heterozygous UTI-KO and wild-type mice were divided into two groups ($n = 10$ each), and were orally administered either TA (purchased from Sigma Chemical Japan, Co, Tokyo, Japan) or vehicle. Animals were killed 20 weeks after the treatment (at 30 weeks of age). Blood samples were collected from all mice, and the serum was separated and stored frozen. Liver lobes were extirpated, and tissues were stored frozen or fixed with 4% paraformaldehyde. TA was mixed in drinking water (300 mg/L) for oral administration in accordance with a previous report.[24] Two groups of five homozygous UTI-KO mice were randomly selected at 26 weeks of age, and underwent surgery under sodium pentobarbital anesthesia (50 mg/kg, intraperitoneally) for implantation of a mini-osmotic pump (model 2004, flow rate of 0.25 $\mu$L/h, maximum total volume of 200 $\mu$L, Alza, Palo Alto, CA, USA). This pump was used to continuously deliver either ulinastatin, UTI agent (10,000 units in 200 $\mu$L solution purchased from Mochida Pharmaceutical Co, Ltd) or vehicle (distilled water) for four weeks. The amount of ulinastatin administered per day was calculated at 357 units, resulting in 12,000 units/kg over the four-week period. Both groups of mice (treated with ulinastatin and control) were killed at 30 weeks of age for measurements of serum liver fibrosis markers and histological examination of liver tissues.

### Assessment of liver fibrosis

Serum levels of HA, a fibrosis marker, were determined at a contract laboratory (SRL Hokkaido, Inc, Hokkaido, Japan). For histological evaluation of liver damage, tissue samples were stained with hematoxylin-eosin and graded according to the criteria reported earlier: 0, no fibrosis; +1, slight fibrosis located in the central liver lobule; +2, moderate wide central fibrosis; +3, severe fibrosis extending to the edge of the liver lobule; and +4, liver cirrhosis.[25] Separately, liver sections were stained with 0.1% Sirius red and 0.1% fast green counterstain (Sigma Chemical Japan) to visualize collagen fibers. Images obtained with a Nikon microscope and DS Camera Control Unit (DS-L1) were quantitatively analyzed according to previously reported procedures utilizing NIH Image software (version 1.62, National Institute of Health, Bethesda, MD, USA) and Adobe® Photoshop image-processing software (Adobe Systems Inc. Japan, Tokyo, Japan).[26-28] $\alpha$-Smooth muscle actin ($\alpha$-SMA) has been advocated as an effective marker for activated stellate cells. We stained activated stellate cells as per the previously described polymer immunocomplex method using mouse monoclonal anti-$\alpha$-SMA antibody (Dako Japan, Tokyo, Japan).[29] Immunohistochemical staining of mouse tissue with mouse monoclonal antibody often results in undesirable background staining because antimouse immunoglobulin secondary antibodies react with endogenously produced mouse immunoglobulin present in the mouse tissue specimen. The polymer immunocomplex staining method eliminates the adverse influence of endogenous mouse immunoglobulin and provides highly specific staining. This method employs a new type of dextran polymer conjugated with secondary antibody having antimouse immunoglobulin specificity (ENVISION, 100-500 $\mu$L/plate, Dako Japan). Polymer immunocomplex is formed by mixing this reagent with mouse monoclonal primary antibody and then with normal immunoglobulin (blocking agent for unbound secondary antibody) at room temperature for one hour. The resulting polymer immunocomplex was added to the mouse tissue sections, which were left standing at 4°C overnight. 3,3'-Diaminobenzidine was used to develop the immunostain. The dextran polymer-based detection reagent (ENVISION or Mouse), normal mouse serum (Code No.X0910), color development substrate (3,3'-diaminobenzidine) and other materials used for immunohistochemical staining in this study were purchased from Dako Japan. Visual fields were randomly chosen from

the stained images, and classified into four groups according to the average proportion of positive cells as described elsewhere (21): 0, no positive cells; (1) positive cells <1/3; (2) positive cells <2/3; and (3) positive cells >2/3. Each plate's score was calculated by taking the mean value of 20 randomly selected visual fields.[25]

### Reverse-transcription PCR

Hepatic mRNA samples were extracted using Sepazol RNA-I (Nacalai Tesque, Kyoto, Japan), and the TGF-$\beta$ expression in liver tissue was determined by reverse-transcription (RT)-PCR using Takara RNA PCR Kit (AMV) version 3.0. The sequences for the upstream and downstream PCR primers for TGF-$\beta$ (PCR product size, 353 bp) were 5′ GCC TGA GTG GCT GTC TTT TGA CG 3′and 5′ ACT TCC AAC CCA GGT CCT TC 3′, respectively. The upstream and downstream PCR primers for $\beta$-actin (PCR product size, 112 bp) had the following sequences, respectively: 5′ TCA GCA AGC AGG AGT ACG ATG A 3′ and 5′ TGC GCA AGT TAG GTT TTG TCA A 3′. The resulting PCR product bands were quantitatively analyzed by using the NIH Image and Adobe® Photoshop software programs.

### Statistics

Data are represented as means ± SD. Repeated measures analysis of variance was used for data analysis, and Duncan's *post hoc* analysis was performed for multiple comparisons. Mann–;Whitney *U* test was used for two-group comparison. *P* values <0.05 were considered statistically significant.

## Results

### The effect of the absence of endogenous UTI on the liver

Liver tissue samples taken from homozygous UTI-KO, heterozygous UTI-KO and wild-type mice were examined by gross observation (Figure 1), hematoxylin–eosin staining (Table 2), Sirius red staining (Figure 2 and Table 3) and $\alpha$-SMA immunohistochemical staining (Table 4) at 30 weeks of age. None of the groups demonstrated liver fibrosis by light microscopic examination. The serum levels of the fibrosis marker HA were compared among the three groups of mice (Table 1). The homozygous UTI-KO group had a higher level of HA than other groups. The wild-type and heterozygous UTI-KO groups had very low levels of hepatic TGF-$\beta$ mRNA expression. The homozygous UTI-KO group demonstrated a higher level of hepatic TGF-$\beta$ mRNA expression than the other two groups. Quantitative RT-PCR analysis demonstrated a significantly higher increase in hepatic TGF-$\beta$ mRNA expression for the homozygous UTI-KO group than the other groups (Figure 3a).

### The effect of continuous UTI administration on the liver

Homozygous UTI-KO mice administered ulinastatin demonstrated a significantly lower level of serum HA than did the control group of homozygous UTI-KO mice

**Figure 1** Typical macroscopic presentations of the liver from UTI-knockout and wild-type mice, treated with or without 20-week administration of thioacetamide. Untreated wild-type and homozygous UTI-knockout (KO) mouse received no drug treatment. The remaining mouse received 300 mg/L thioacetamide (TA) in their drinking water for the final 20 weeks of the experiment. (a) Untreated wild-type mouse, 30 weeks of age. (b) Untreated homozygous UTI-KO mouse, 30 weeks of age. (c) Treated wild-type mouse, 30 weeks of age. (d) Treated homozygous UTI-KO knockout mouse, 30 weeks of age. UTI, urinary trypsin inhibitor

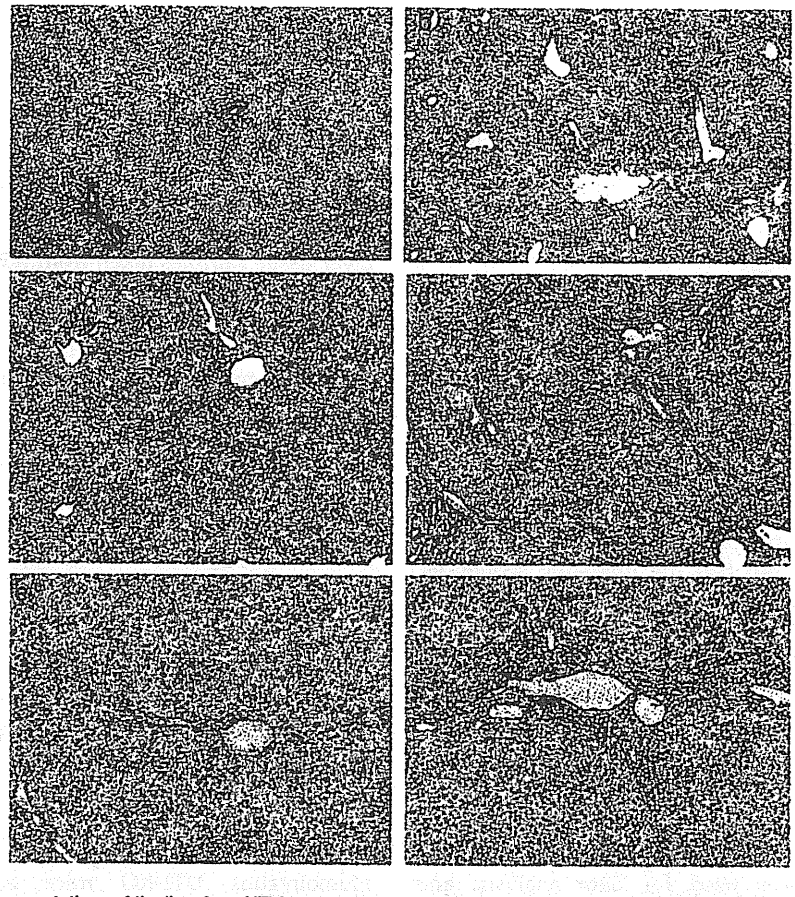

Figure 2 Typical histological presentations of the liver from UTI-knockout and wild-type mice, treated with or without 20-week administration of thioacetamide. Untreated wild-type and homozygous UTI-knockout (KO) mouse received no drug treatment. The remaining mouse received 300 mg/L thioacetamide (TA) in their drinking water for the final 20 weeks of the experiment. The sections were stained with Sirius red to detect the extracellular matrix and collagen. Activated hepatic stellate cells were detected by immunohistochemistry with a monoclonal antibody for $\alpha$-smooth muscle actin ($\alpha$-SMA). (a) Untreated wild-type mouse, 30 weeks of age, Sirius red staining (×40). (b) Untreated homozygous UTI-KO mouse, 30 weeks of age, Sirius red staining (×40). (c) Treated wild-type mouse, 30 weeks of age, Sirius red staining (×100). (d) Treated homozygous UTI-KO mouse, 30 weeks of age, Sirius red staining (×100). (e) Treated wild-type mouse, 30 weeks of age, $\alpha$-SMA immunohistochemical staining (×100). (f) Treated homozygous UTI-KO mouse, 30 weeks of age, $\alpha$-SMA immunohistochemical staining (×100). UTI, urinary trypsin inhibitor

administered distilled water (Table 1). In addition, quantitative RT-PCR analysis showed that TGF-$\beta$ expression was significantly suppressed in homozygous UTI-KO mice continuously administered ulinastatin than in homozygous UTI-KO mice administered vehicle only (Figure 3b).

### Development of TA-induced liver fibrosis

Administration of TA induced a significant increase in serum HA in all three groups. However, the homozygous UTI-KO group showed a significantly higher increase in serum HA than did the heterozygous UTI-KO and wild-type groups (Table 1). In addition, TA-induced liver fibrosis was macroscopically observed in all groups; however, liver cirrhosis was more severe in the homozygous UTI-KO group than the other two groups. Homozygous UTI-KO mice demonstrated macroscopically observable irregular nodules on the entire liver surface, which indicated severe cirrhotic changes. Moreover, Sirius red staining revealed that these mice developed thick fibrous septae that formed pseudolobules, indicating severe cirrhotic changes (Figures 1 and 2). According to the histological analysis based on hematoxylin–eosin staining (Table 2), Sirius red staining (Figure 2 and Table 3) and $\alpha$-SMA immunohistochemical staining (Table 4), the homozygous UTI-KO group consistently scored significantly higher (indicating more adverse changes) than did the other groups. With respect to TGF-$\beta$ mRNA, strong hepatic expression was found in all groups. However, the homozygous UTI-KO group showed a significantly higher increase in TGF-$\beta$ expression than did the other groups (Figure 3c).

## Discussion

TGF-$\beta$ is produced in its latent form by stellate cells, Kupffer cells and platelets, and is converted to its active form by proteases.[12,30–34] It has been clearly documented that the conversion of latent to active TGF-$\beta$ in the liver requires a serine protease.[12,29] In particular, the serine protease plasmin has been shown to play a key role in TGF-$\beta$ activation during the development of liver fibrosis and cirrhosis. Another common protease, kallikrein, is known to

**Table 1** Serum hyaluronic acid (HA) levels

| | n | HA (ng/mL) |
|---|---|---|
| Wild | 10 | 236.4 ± 23.3 |
| Hetero | 10 | 241.6 ± 22.4 |
| Homo | 10 | 436.6 ± 39.6* |
| TA + wild | 10 | 1039.3 ± 104.8† |
| TA + hetero | 10 | 1081.5 ± 260.4‡ |
| TA + homo | 10 | 2236.1 ± 283.5§,** |
| Ulinastatin + homo | 5 | 296.4 ± 28.6¶ |
| Vehicle + homo | 5 | 438.4 ± 53.2 |

TA, thioacetamide; HA, hyaluronic acid; UTI, urinary trypsin inhibitor; homo, homozygous UTI-KO mouse; hetero, heterozygous UTI-KO mouse
Wild, wild-type mouse, 30 weeks of age; hetero, heterozygous UTI-knockout (KO) mouse, 30 weeks of age; homo, homozygous UTI-KO mouse, 30 weeks of age; TA + wild, wild-type mouse, 30 weeks of age, after 20-week administration of thioacetamide (TA); TA + hetero, heterozygous UTI-KO mouse, 30 weeks of age, after 20-week administration of TA; TA + homo, homozygous UTI-KO mouse, 30 weeks of age, after 20-week of administration of TA; ulinastatin + homo, homozygous UTI-KO mouse with four-week continuous intraperitoneal administration of ulinastatin; vehicle + homo, homozygous UTI-KO mouse with four-week continuous intraperitoneal administration of distilled water. Data are represented as mean ± SD. The column headed by '*n*' indicates the numbers of mice tested.
*$P < 0.01$ versus wild and hetero groups, †$P < 0.01$ versus wild group, ‡$P < 0.01$ versus hetero group, §$P < 0.01$ versus homo group, **$P < 0.01$ versus TA + wild and TA + hetero groups and ¶$P < 0.05$ versus vehicle + homo group

**Table 2** Pathological grading of liver fibrosis based on hematoxylin–eosin-stained samples

| | *n* | 0 | 1 | 2 | 3 | 4 | Average score |
|---|---|---|---|---|---|---|---|
| Wild | 10 | 10 | 0 | 0 | 0 | 0 | 0 |
| Hetero | 10 | 10 | 0 | 0 | 0 | 0 | 0 |
| Homo | 10 | 10 | 0 | 0 | 0 | 0 | 0 |
| TA + wild | 10 | 0 | 0 | 3 | 5 | 2 | 2.9 ± 0.2 |
| TA + hetero | 10 | 0 | 0 | 3 | 6 | 1 | 2.8 ± 0.2 |
| TA + homo | 10 | 0 | 0 | 0 | 2 | 8 | 3.8 ± 0.1* |

TA, thioacetamide; UTI, urinary trypsin inhibitor; homo, homozygous UTI-KO mouse; hetero, heterozygous UTI-KO mouse
Wild, wild-type mouse, 30 weeks of age; hetero, heterozygous UTI-knockout (KO) mouse, 30 weeks of age; homo, homozygous UTI-KO mouse, 30 weeks of age; TA + wild, wild-type mouse, 30 weeks of age, after 20-week administration of thioacetamide (TA); TA + hetero, heterozygous UTI-KO mouse, 30 weeks of age, after 20-week administration of TA; TA + homo, homozygous UTI-KO mouse, 30 weeks of age, after 20-week of administration of TA. Data are represented as mean ± SD. The column headed by '*n*' indicates the numbers of mice tested
*$P < 0.01$ versus TA + wild and TA + hetero groups

activate TGF-β when liver regeneration is impaired.[12,35] We maintain that endogenous UTI suppresses TGF-β activation and liver fibrosis, independent of hepatic pathology type, because it inhibits a large number of serine proteases and other proteases. Analysis of the individual effects of UTI on these proteases was, however, beyond the scope of the

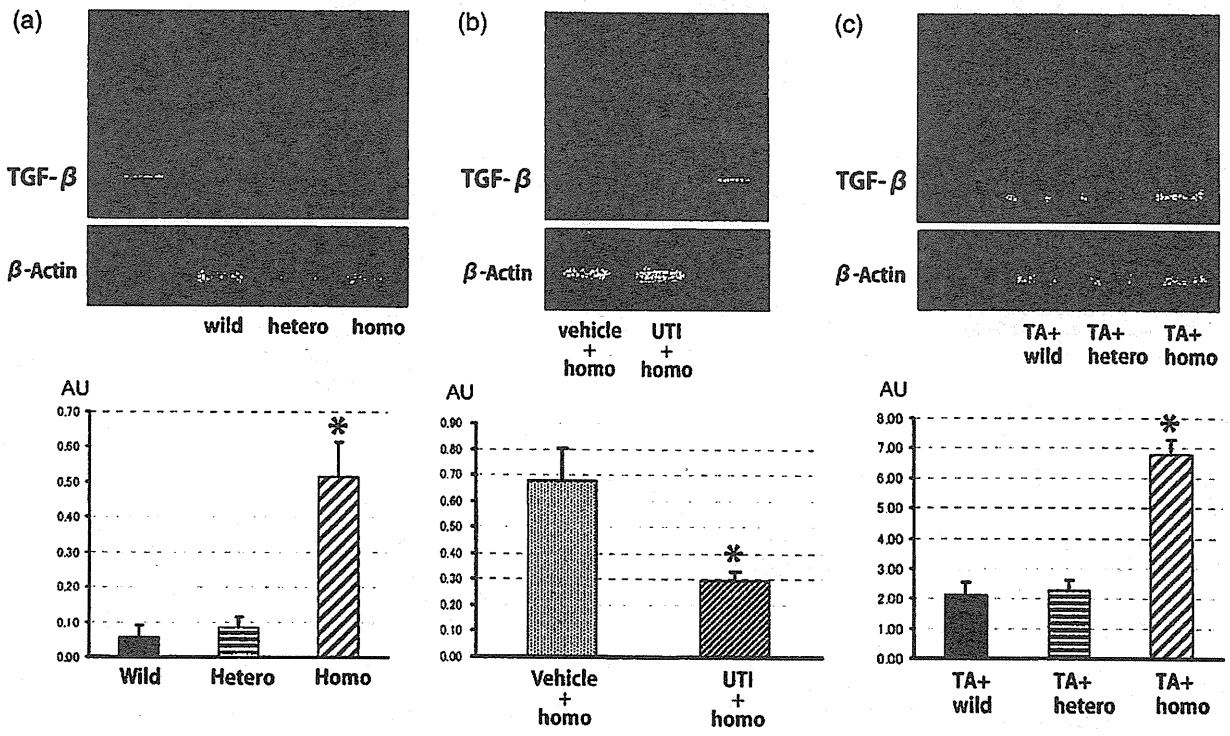


**Figure 3** Typical presentations of PCR products for TGF-β mRNA extracted from UTI-knockout and wild-type mice. (a) Wild, wild-type mouse, 30 weeks of age; hetero, heterozygous UTI-knockout (KO) mouse, 30 weeks of age; homo, homozygous UTI-KO mouse, 30 weeks of age. *$P < 0.01$ versus wild and hetero. (b) Two groups of five homozygous UTI-KO mice received continuous intraperitoneal administration of either ulinastatin, UTI agent (12,000 units/kg/d) or vehicle (distilled water) for four weeks using a mini-osmotic pump. Vehicle + homo, homozygous UTI-KO mouse treated with vehicle; UTI + homo, homozygous UTI-KO mouse treated with ulinastatin. *$P < 0.05$ versus vehicle + homo. (c) The mouse, 30 weeks of age, received 300 mg/L thioacetamide (TA) in their drinking water for the final 20 weeks of the experiment. TA + wild, wild-type mouse; TA + hetero, heterozygous UTI-KO mouse; TA + homo, homozygous UTI-KO mouse. *$P < 0.05$ versus TA + wild and TA + hetero. AU: Arbitrary units denote the band density ratio of the target gene relative to β-actin. Data are represented as means ± SD ($n = 5$)UTI, urinary trypsin inhibitor; PCR, polymerase chain reaction; TGF-β, transforming growth factor-β

**Table 3** Pathological grading of liver fibrosis based on Sirius red-stained samples

| | *n* | Sirius red matrix density (%) |
|---|---|---|
| Wild | 10 | 0 |
| Hetero | 10 | 0 |
| Homo | 10 | 0 |
| TA + wild | 10 | 11.1 ± 1.4* |
| TA + hetero | 10 | 10.8 ± 1.2* |
| TA + homo | 10 | 21.3 ± 2.1*,† |

TA, thioacetamide; UTI, urinary trypsin inhibitor; homo, homozygous UTI-KO mouse; hetero, heterozygous UTI-KO mouse
Wild, wild-type mouse, 30 weeks of age; hetero, heterozygous UTI-knockout (KO) mouse, 30 weeks of age; homo, homozygous UTI-KO mouse, 30 weeks of age; TA + wild, wild-type mouse, 30 weeks of age, after 20-week administration of thioacetamide (TA); TA + hetero, heterozygous UTI-KO mouse, 30 weeks of age, after 20-week administration of TA; TA + homo, homozygous UTI-KO mouse, 30 weeks of age, after 20-week administration of TA. Data are represented as mean ± SD. The column headed by '*n*' indicates the numbers of mice tested.
*$P < 0.01$ versus wild, hetero and homo groups, respectively. †$P < 0.01$ versus TA + wild and TA + hetero groups

**Table 4** Evaluation of the activation of stellate cells based on immunohistochemical staining of α-smooth muscle actin

| | *n* | 0 | 1 | 2 | 3 | Average score |
|---|---|---|---|---|---|---|
| Wild | 10 | 10 | 0 | 0 | 0 | 0 |
| Hetero | 10 | 10 | 0 | 0 | 0 | 0 |
| Homo | 10 | 10 | 0 | 0 | 0 | 0 |
| TA + wild | 10 | 0 | 3 | 6 | 1 | 1.8 ± 0.2* |
| TA + hetero | 10 | 0 | 2 | 5 | 3 | 2.1 ± 0.2* |
| TA + homo | 10 | 0 | 0 | 1 | 9 | 2.9 ± 0.1*,† |

TA, thioacetamide; UTI, urinary trypsin inhibitor; homo, homozygous UTI-KO mouse; hetero, heterozygous UTI-KO mouse.
Wild, wild-type mouse, 30 weeks of age; hetero, heterozygous UTI-knockout (KO) mouse, 30 weeks of age; homo, homozygous UTI-KO mouse, 30 weeks of age; TA + wild, wild-type mouse, 30 weeks of age, after 20-week administration of thioacetamide (TA); TA + hetero, heterozygous UTI-KO mouse, 30 weeks of age, after 20-week administration of TA; TA + homo, homozygous UTI-KO mouse, 30 weeks of age, after 20-week of administration of TA. Data are represented as mean ± SD. The column headed by '*n*' indicates the numbers of mice tested
*$P < 0.01$ versus wild, hetero and homo groups, respectively. †$P < 0.01$ versus TA + wild and TA + hetero groups

present study. Such analysis will be the focus of future studies.

In the present study, we employed UTI-KO mice and investigated the various roles of endogenous UTI in the process of liver fibrosis. To the best of the authors' knowledge, the present study was the first to investigate the mechanisms of liver fibrosis in endogenous UTI-KO mice. The use of genetically engineered animals is an extremely useful method for investigating the effects of endogenous factors possibly involved in the development of liver fibrosis.[27,36] Our interest focused on the physiological functions of endogenous UTI in the liver, in particular its suppressive potential against liver fibrosis.

Various nutrients absorbed through the intestinal mucous membrane have been documented to reach the liver via the portal vein. A small amount of bacterial toxins from the decomposition of dead bacteria in the intestinal flora has been reported to enter the liver via the portal vein as well.[37–39] Moreover, cirrhotic patients are continuously exposed to a low concentration of endotoxin.[40,41] These facts suggest that the liver is at a constant risk of being injured by factors of external and internal origin, even in healthy individuals. Such injuries can potentially cause liver fibrosis.[11,42] In this study, concentrations of hepatic TGF-β and serum hyaluronic acid (a surrogate measure for liver fibrosis) were elevated in the endogenous UTI-KO mice and were suppressed by administration of exogenous UTI, ulinastatin. Moreover, in our experiment with TA-induced liver fibrosis using KO mice unable to produce UTI in the liver, homozygous UTI-KO mice showed a significantly higher degree of liver fibrosis than did heterozygous UTI-KO and wild-type mice. These results strongly suggest that the liver possesses a self-protective mechanism whereby it inhibits the development of fibrosis through endogenous production of UTI that suppresses the production and protease-induced activation of TGF-β. However, our study results require careful scrutiny, as they failed to demonstrate that the biological profiles of all other endogenous substances involved in liver fibrosis were similar between the genetically engineered and wild-type mice. TGF-β induces an increase in hepatic collagen α1(I) expression;[7,10] therefore, verification of hepatic collagen α1(I) expression in homozygous UTI-KO mice would verily provide strong evidence; however, we have not performed this verification yet. Another possibility is an unidentified fibrosis-suppression mechanism acting in a fail-safe manner, thus preventing the development of fibrosis in UTI-KO mice. These possible mechanisms merit future research.

TA-induced murine liver fibrosis has been shown to present with pathological characteristics similar to chronic hepatitis C infection and liver cirrhosis in humans.[24,43,44] One of the limitations of the present study was that we did not demonstrate the antifibrotic effect of exogenous UTI in TA-induced liver fibrosis in UTI-KO mice. A previous study using a rat model of swine serum-induced liver fibrosis found that the protease inhibitor camostat mesilate had inhibition potential similar to that of UTI in its suppression of plasmin-dependent TGF-β activation, and demonstrated that this protease inhibitor was a promising drug candidate for the treatment of liver fibrosis.[14]

In preliminary experiments using the mini-osmotic pump system in TA-treated homogenous UTI-KO mice, we failed to demonstrate that TA-induced TGF-beta up-regulation and liver fibrosis progression were suppressed by continuous infusion of ulinastatin. Since the plasma half-life of UTI is a mere 35 min,[4] a larger dose of ulinastatin over a longer period by repeated or continuous administration was possibly required to establish UTI's antifibrotic action. Such dose adjustment is one of the multiple difficulties that we must address before we can succeed in applying ulinastatin to the clinical treatment of liver fibrosis.

UTI is covalently linked to one or two polypeptides, referred to as heavy chain (HC) 1, HC 2, and HC3, via a chondroitin sulfate chain.[45] Homogenous UTI-KO mice showed no expression of UTI as well as HCs.[23] The HCs are also known as serum-derived hyaluronan-associated proteins (SHAPs).[46] SHAPs covalently bind to hyaluronan